

## Extreme disorder-phonon competition and liquid-like thermal conduction in AgCrSe<sub>2</sub>

Thermal transport is one of the most fundamental properties of matter. Materials with small thermal conductivity are desirable for a great diversity of applications such as thermal insulation, optical phase-change memory devices and efficient thermoelectric energy conversion [1]. Thus, a persistent challenge is to reduce the thermal conductivity of solids as much as possible. In general, acoustic phonons of solids are the major heat-carriers so that several strategies are proposed to enhance the scattering of acoustic phonons for suppressing thermal conduction, such as disorder scattering, anharmonic phonon interactions, uncorrelated or concerted rattling modes, interfaces and grain boundaries [1]. Disorder-phonon coupling has been frequently employed to achieve ultralow thermal conductivities in leading thermoelectrics, for example, Zn<sub>4</sub>Sb<sub>3</sub> [2] and Cu<sub>2</sub>Se [3]. It is true that the thermal conduction can be effectively suppressed in this way, but it still remains unknown that to what extent the acoustic phonons can be scattered. Such an issue is also fundamentally critical, given that it may define the physical lower limit of thermal conductivity in solids.

It is known that AgCrSe<sub>2</sub> undergoes a superionic transition at  $T_C$  of about 450 K, above which Ag ions become disordered, with high ionic conductivity [4]. In order to examine the atomic structures, we performed high-energy X-ray diffraction at SPing-8 BL04B2. The obtained diffraction data,  $S^X(Q)$ , were converted into pair distribution function,  $G^X(r)$ , in real space.

AgCrSe<sub>2</sub> crystallizes in a hexagonal structure with alternative Ag layers and CrSe<sub>6</sub> octahedral layers repeating along the  $c$  axis, as shown in Fig. 1(a). Ag atoms lie in the equivalent tetrahedral interstitial sites in between CrSe<sub>6</sub> layers. In the ground state, it

is expected that only one specific site is fully occupied and as temperature rises, an increasing number of Ag ions immigrate to another site owing to the jump diffusion. At  $T_C$  of about 450 K, the occupation of Ag ions undergoes an order-to-disorder transition to the high-temperature phase with 50% occupation at each site while the space group of crystal symmetry changes from  $R3m$  to  $R\bar{3}m$ . The crystallographic changes are evidenced at X-ray scattering structure factor  $S^X(Q)$  by the disappearance of Bragg peaks (003) and (006) as well as the weakening of (105), as shown in the inset of Fig. 1(b).

Shown in Fig. 2(a) are  $G^X(r)$  at selected temperatures. The uniform nearest neighboring Ag–Ag distance splits into three sets due to the occupational disorder and the next nearest neighboring Ag-related correlations sequentially become diverse as well. This is responsible for the special temperature dependence of  $G^X(r)$ . With the guide of the partial PDF of Ag-related correlations shown in the lower part of Fig. 2(a), it can be seen that heights of Ag-related peaks are much more susceptible to the change of temperature, such as those at 4.5, 13 and 19 Å. As a representative, the integrated intensity of the peak at 4.5 Å is plotted in Fig. 2(b), which exhibits a well-defined critical-like behavior, in contrast to the 3.5 Å peak where contributions of Ag-related pairs are marginal. It is suggested that the disorder of atomic occupation of silver is saturated above  $T_C$ .

The occupational disorder has a direct influence on atomic dynamics because the transverse acoustic (TA) phonons are exclusively contributed by atomic motions of silver (Fig. 3(d)). In other words, there is a maximized competition between the local and global atomic motions. At higher temperatures, the

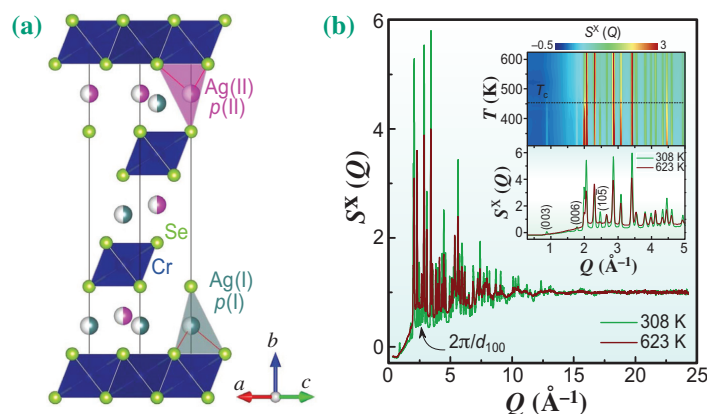


Fig. 1. (a) The crystal structure of AgCrSe<sub>2</sub>. (b) The structure factor,  $S^X(Q)$ , obtained in X-ray scattering at 308 and 623 K. The diffuse scattering appears at about 2.0 Å<sup>-1</sup>. The inset highlights  $S^X(Q)$  at the small- $Q$  region for temperature evolution (upper) and two end temperatures (lower).

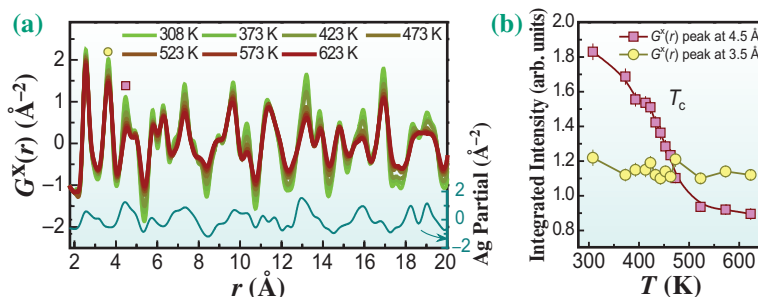


Fig. 2. (a) The experimental X-ray PDF,  $G^X(r)$ . Underneath is the superposition of partial  $G^X(r)$  for Ag-involved pairs calculated on the  $R3m$  crystal model. (b) The integrated intensity of  $G^X(r)$  for the Ag-correlation-poor peak at 3.5 Å and the Ag-correlation-rich peak at 4.5 Å, which are labeled by a circle and a square in (a), respectively.

system is dominated by the local dynamics so that it is understandable that the global counterpart vanishes. Figure 3(a) and b shows inelastic neutron scattering  $S(Q, E)$  with incident energy ( $E_i$ ) of 5.931 meV at 150 and 520 K, respectively. It can be seen that pronounced diffuse scattering exists at  $Q \sim 2.0 \text{ \AA}^{-1}$ . At 150 K, the diffuse scattering appears just in the vicinity of the elastic line and TA phonons are fairly sharp. Nevertheless, the diffuse scattering becomes dominant at 520 K at the expense of Bragg peaks and TA phonons. Their evolution as a function of temperature

is plotted in Fig. 3(c). TA phonons are softened and gradually merged into the diffuse scattering around  $T_c$ .

It is well-known that a solid conducts heat through both transverse and longitudinal acoustic phonons, but a liquid employs only longitudinal vibrations. As a result, a solid is usually thermally more conductive than a liquid. The present observation provides a unique example where a solid mainly conducts heat via longitudinal acoustic phonons. Moreover, it has important implications on tailoring the properties of thermoelectrics [5].

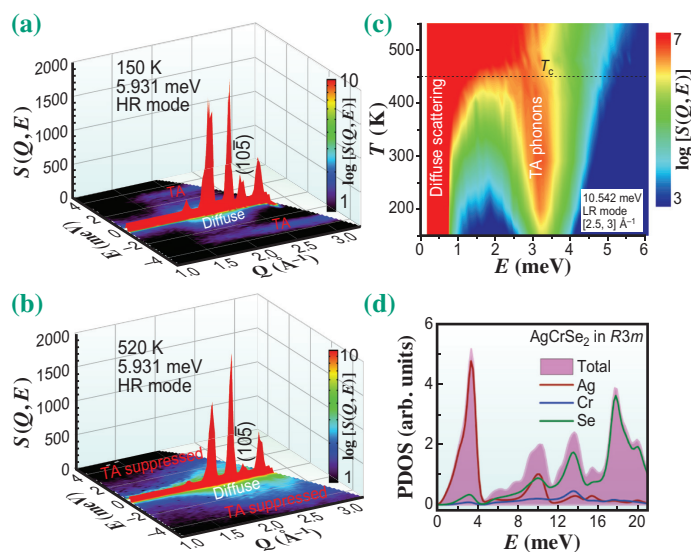


Fig. 3. (a) and (b)  $S(Q, E)$  surface plots at 150 and 520 K at  $E_i = 5.931 \text{ meV}$  obtained in inelastic neutron scattering measurements performed at AMATERAS of J-PARC. (c) Contour plot of  $S(Q, E)$  as a function of temperature with  $E_i = 10.542 \text{ meV}$  at  $Q$  of  $[2.5, 3] \text{ \AA}^{-1}$ . (d) Calculated phonon density of state (PDOS) of  $\text{AgCrSe}_2$  in  $R3m$ .

Bing Li

Institute of Metal Research,  
Chinese Academy of Sciences, China

Email: bingli@imr.ac.cn

### References

- [1] J.G. Snyder and E.S. Toberer: *Nat. Mater.* **7** (2008) 105.
- [2] G.J. Snyder *et al.*: *Nat. Mater.* **3** (2004) 458.
- [3] H. Liu *et al.*: *Nat. Mater.* **11** (2012) 422.
- [4] D.W. Murphy and H.S. Chen: *J. Electrochem. Soc.* **124** (1977) 1268.
- [5] B. Li, H. Wang, Y. Kawakita, Q. Zhang, M. Feyngenson, H.L. Yu, D. Wu, K. Ohara, T. Kikuchi, K. Shibata, T. Yamada, X.K. Ning, Y. Chen, J.Q. He, D. Vaknin, R.Q. Wu, K. Nakajima and M.G. Kanatzidis: *Nat. Mater.* **17** (2018) 226.